Nuclear Instruments and Methods in Physics Research A 593 (2008) 431–439

Contents lists available at ScienceDirect

Nuclear Instruments and Methods in Physics Research A

journal homepage: www.elsevier.com/locate/nima

Design concept and modeling of a new Positron Identification by Coincident Annihilation Photons (PICAP) system

J.J. Connell [*,1], J.R. Kalainoff [1,2], C. Lopate [1]

Space Science Center, University of New Hampshire, Durham, NH 03824, USA

ARTICLE INFO

Article history:
Received 23 July 2007
Received in revised form
10 May 2008
Accepted 25 May 2008
Available online 1 June 2008

Keywords:
Cosmic ray instruments
Solar energetic particle instruments
Positron instruments
Spacecraft instruments

ABSTRACT

The Positron Identification by Coincident Annihilation Photons (PICAP) system is a new design concept to measure moderate energy (~few MeV) positrons and negatrons in space. Positron measurements in this energy range would open a window on cosmic ray propagation in the Galaxy, Solar modulation of cosmic rays (particularly charge-sign effects) and Solar energetic particles. Electrons of both charge signs are first identified by the conventional dE/dx versus residual energy technique. Coincident 511 keV annihilation photons are used to identify stopping positrons. This technique is far simpler than magnet spectrometers, which require elaborate tracking systems and associated electronics. We present a baseline design and Monte-Carlo modeling results using EGS4. We estimate the baseline instrument would mass ~4 kg and use ~3 W of power making such an instrument highly attractive for resource-constrained space missions.

1. Introduction

We report on a design concept and computer modeled response of an innovative and simple detector system to identify moderate energy (a few MeV) positrons in space. This detector scheme, which we call the Positron Identification by Coincident Annihilation Photons (PICAP) system, is based upon simple, reliable, well-proven and robust detectors. A PICAP instrument would be particularly attractive as to cost, mass, power and telemetry requirements. It would be well suited to a variety of space missions, including deep space missions, in contrast to more complex and massive magnetic spectrometer techniques.

The limited resources on spacecraft place severe constraints on instrument mass, power and telemetry. This is particularly true where an experiment is crucial to the science goals of a mission, but is not the main instrument on the spacecraft. A PICAP instrument would be useful as a charged particle instrument on such missions as the proposed NASA Telemachus, Heliospheric Imager and Galactic Observer (HIGO), Solar Sentinels, Solar Probe, Interstellar Probe, Particle Acceleration Solar Orbiter (PASO) or ESA's Solar Orbiter. We estimate that an effective PICAP instrument can be built with a mass of about 4 kg and a power usage of about 3 W.

Most positron measurements to date have been made at higher energies using magnet spectrometers; there is no intrinsic reason this technique cannot be extended to lower energies, though multiple scattering effects become an increasing concern with decreasing energy. Unfortunately, a magnet spectrometer would mass 10 kg or more. It would also require a complex multiple trajectory determining system with support electronics that would typically use >10 W of power. A PICAP instrument would thus be far less massive and use significantly less power than a magnet spectrometer, enhancing its attractiveness for future flight opportunities. Furthermore, the presence of a magnet aboard a spacecraft, even one with a minimal fringe field, can cause significant difficulties for other instruments, particularly magnetometers. A PICAP instrument has no magnet, making it fully compatible with any other flight instruments.

While the primary goal is measuring positrons, a PICAP instrument can also be used to study ions and would have some sensitivity to γ-rays and neutrons.

2. Scientific motivation for positron measurements in space

The detection and identification of moderate and high-energy electrons (in this paper, we use "electrons" to mean both negatrons, e^-, and positrons, e^+) is essential to studies of space radiation. Aside from albedo from cosmic ray interactions with planetary bodies, which are significant only near such bodies, there are two main sources of positrons in the Heliosphere: Galactic cosmic rays (GCRs) and transient Solar energetic particle

* Corresponding author. Tel.: +1 603 862 5096; fax: +1 603 862 3584.
E-mail address: james.connell@unh.edu (J.J. Connell).
[1] Also Department of Physics.
[2] Currently United States Army.

0168-9002/$ - see front matter © 2008 Elsevier B.V. All rights reserved.
doi:10.1016/j.nima.2008.05.051

(SEP) events. Measurement of the positron fraction in GCRs in the $\sim$1 to $\sim$50 MeV energy interval would provide a valuable window on cosmic ray propagation and modulation; similarly, measurement of the positron fraction in SPEs would provide a new tool to help understand the acceleration processes near the Sun.

At higher energies ($>$50 MeV), these goals will be met by the recently launched PAMELA (Payload for Antimatter Matter Exploration and Light-nuclei Astrophysics) instrument. PAMELA, however, is very large (470 kg, 355 W) and in an elliptical (360×600 km) highly inclined (70°) low Earth orbit [1]. Measurements of moderate energy electrons will require much higher orbits, preferably beyond the Earth's magnetosphere. The resource requirements of a PAMELA-scale instrument would be challenging for any mission beyond low Earth orbit, and would be effectively prohibitive for a deep space mission.

At lower energies, we are aware of only a few positron measurements:

In 1973, Hurford et al. [2] and in 1975, Mewaldt et al. [3] reported on lower limits for positrons in the 0.2–2 MeV energy interval using the Electron/Isotope Spectrometers (EIS) on IMP-7 and -8. These instruments were Si solid-state detector stacks surrounded by scintillator anti-coincidence shields. The technique was, in essence, similar to PICAP: electrons were identified by dE/dx and residual energy measurements; positrons were identified among the electrons by detection of a single annihilation photon in a Si detector. Si is not a good detector for γ-rays, and the efficiency for detecting positrons was 1.6–0.28%, depending on where the positron stopped and annihilated in the stack. The EIS instruments were not principally designed to detect positrons. Our baseline PICAP instrument efficiency for single-photon positron detections is $\sim$10% while the cleaner two-photon detection efficiency is $\sim$1%. The EIS measurements placed an upper limit of $<6 \times 10^{-3}$ on the positron fraction in the 0.2–2 MeV energy range for a number of Solar flares. As the authors point out, in this energy interval inverse-β decay isotopes would be the dominant source of positrons, as opposed to pion production at slightly higher energies (see Section 2.3).

In 1969, Cline and Porreca [4] reported on positron measurements in the 2–9.5 MeV energy interval. As with the previous measurement, the instrument first identified electrons using a single dE/dx versus residual energy technique. In the case of OGO-5, both measurements were made using plastic scintillator. A CsI crystal scintillator detecting single 511 keV photons was used to identify positron events. The OGO-5 instrument was better suited to positrons measurements than the EIS instruments owing the larger mass, and higher photon detection efficiency, of the CsI crystal compared to Si detectors. (The detection efficiency for annihilation photons was stated as a few percent.) The instrument also benefited from being on a boom, reducing background effects from the spacecraft. The measurements reported were for quiet time GCRs, not SEP events. The measured positron fraction was 1.8 ± 0.2%.

Also in 1969, Cline and Hones [5] reported on results from an instrument on OGO-3. The measurement was for energies of $\sim$1 MeV. This instrument looked for electrons stopping in a scintillator partially surrounded by an anti-coincidence scintillator shield. Positrons were identified using two CsI detectors. This instrument is interesting in that it, like PICAP, looked for two annihilation photons. PICAP differs in that it identifies electron based on multiple dE/dx versus residual energy, whereas the OGO-3 instrument only measured the residual energy of stopping particles. The OGO-3 instrument also had a very limited active shielding compared to a PICAP instrument.

In 1985, Kirsch et al. reported a possible detection of positrons for a Solar flare on June 3, 1982 using the medium energy charged particle spectrometer E8 on Helios-1 [6]. This instrument used an inhomogeneous field from a permanent magnet to separate and focus electrons onto solid-state detectors [7]. The positron channels included active anti-coincidence detectors, but in the presence of large penetrating proton, neutron or photon fluxes, the positron channels were dominated by background. The measurement was therefore based upon a precursor to the arrival of the flare protons. The timing was consistent with positrons. After background subtraction, the detection was for 17 ± 14 positrons, corresponding to a flux of 0.88 $e^+/(cm^2\,sr\,s)$ at 0.57 AU in the 152–546 keV energy interval. The authors extrapolate to a flux of 0.28 $e^+/(cm^2\,sr\,s)$ at 1 AU. The conclusion was that $<\sim$10% of positrons escape into the interplanetary medium. The energy was well below that of a PICAP instrument, and as with the EIS energy interval, inverse-β decay isotopes would be the dominant positron production mechanism.

Compared to the instruments described earlier, PICAP uses multiple dE/dx measurements (as in the IMP instruments) with the detection of pairs of 511 keV photons (as in OGO-3). It thus combines the more stringent identification of electrons (both negatrons and positrons are separated from the large proton background) with the more stringent identification of positrons (as differentiated from negatrons).

2.1. Galactic cosmic ray electrons

Positrons have long been known to form a component of GCRs (e.g. Refs. [8,9]). The bulk of cosmic ray positrons are secondary in origin. In common with anti-protons, secondary positrons probe the propagation history of the most abundant cosmic ray species—protons. This is in contrast with such secondary species as B and the sub-Fe group, which are predominantly products of heavier primary species. The dominant channel of positron production is via π^+ production when cosmic ray protons interact with the interstellar medium (ISM). As this results in a much lower threshold than for anti-proton production, positrons provide information about the propagation of lower energy cosmic ray protons. There are some contributions to the low energy positron spectrum expected from the decay of nucleosynthetically created radionuclides in supernovae, cosmic-ray secondary β^+ radionuclides and pair production near black holes and neutron stars. Some theories of dark matter and topological defects also predict a primary positron component. In order to separate any such primary sources, it is first critical to understand the secondary production.

There are several models for cosmic ray propagation through the Galaxy, each of which makes different predictions for the propagation of positrons in the Galaxy. These different models of cosmic ray confinement in our Galaxy (e.g. leaky box models, nested leaky box models, diffuse halo models, dynamic halo models, closed Galaxy models and others) all predict positron fractions that vary with energy. At low energies, these model predictions often diverge; reliable measurements would constrain these models. As there have been few measurements of positrons below $\sim$100 MeV, model predictions have not generally extended to those low energies, but extrapolations of the model prediction from 100 down to 10 MeV indicate that the expected positron fraction should vary from model to model by factors of two to four, which is the same order of variation expected at GeV energies (e.g. Ref. [10]). Not only would a positron fraction measurement at 10 MeV significantly extend the energy range over which observations have been made, a sufficiently accurate measurement of the positron fraction in the low energy cosmic rays will help distinguish between these cosmic ray confinement models.

Studies of proton secondaries (positrons and anti-protons) are particularly direct in their implications for, and relationship with, Galactic γ-ray background models [11]. In these models, positron measurements have been important in constraining the spectral index of the comic ray source and the role of reacceleration in the Galaxy.

2.2. Charge-sign effects in cosmic ray modulation

In order to fully understand our Heliosphere, we must understand how charged particles move in the Solar wind plasma, which fills the Heliosphere. The general structure of the Heliospheric plasma and magnetic fields, which control charged particle transport, were laid out by Parker [12]. Solar modulation theories continued to increase in detail when the first explanation of all the modulation effects, as we think of them today, were described [13]. Of major importance was the fact that the drift of charged particles in the Heliosphere was expected to have a significant role in overall modulation. Predictions of the effects of drifts in cosmic ray flux time–intensity profiles [14] immediately followed.

In order to test the predictions of drifts on cosmic ray modulation, researchers turned to charge-sign effects. It was noted that simultaneously measurements of electrons and positively charged ions, the general predictions of Jokipii et al. [13] were observed; however, the electron peaks during the Solar minima of A+ cycles were never as sharp nor the plateaus seen during the Solar minima of A− cycles ever as broad as those observed for positively charged particles (e.g. Ref. [15]). Also, some electron measurements made during the 1987 Solar minimum showed an unusual recovery, to about 30% above any previous (or subsequent) measurement [16]. However, studies of charge-sign dependencies of Heliospheric modulation have almost always been made comparing either protons and/or helium with electrons. The energy intervals are generally chosen so that particles with similar rigidity can be compared, for example 1.2 GeV electrons versus 190 MeV/nucleon helium—having total rigidities of $\sim$1.20 and $\sim$1.25 GV, respectively. These types of comparisons are compromised by the fact that the two species have very different velocities—$\sim$1.0 and $\sim$0.5 c, respectively, for the immediate example. Thus, there is a critical question as to how much of the difference in the observed time–intensity profiles is due to charge-sign effects and how much is due to velocity dependent effects in Solar modulation. Also, the possibility that the electron measurements were not completely negatrons, but had some positron contamination, added to the difficulty in unambiguously distinguishing charge-sign effects.

The possibility of a single instrument simultaneously measuring positrons and negatrons would address many of the problems in charge-sign calculations. As the positrons and negatrons would have the same energy, and of course the same mass, both the rigidity and velocity of these particles would be identical. One would not have the problem of trying to untangle these quantities for modeling efforts. The PICAP method of particle identification means that the *negatron* flux, as opposed to the *electron* (combined negatron and positron) flux, can be determined. The recent launch of PAMELA aside [1], most measurements of GCR positrons have come from sub-orbital balloon missions. If the measurements are made with a spacecraft instrument (rather than a balloon package), the charge-sign dependence could be monitored continuously. One would no longer have to worry that a large transient event could occur during a balloon flight and distort the measurements. The long duration of space missions as compared to balloon flights (years rather than weeks) would allow for a positron fraction measurement with high statistical precision, thus allowing detection of small charge-sign effects. Finally, the continuous monitoring would allow the study of short-term variations in the charge-sign dependence, rather than looking only for long-term changes.

There has been some modeling of the differences in response that might exist between positrons and electrons accelerated at shocks found in co-rotating interaction regions (CIRs) that suggest that the positron/electron ratio might be an indicator of drift effects in the foreshock region [17,18]. Because the CIR particle acceleration would occur at lower Heliographic latitudes, the oppositely charged particles would drift in opposite directions in the foreshock region, and thus encounter the shock at different Heliographic longitudes. The model predicts that the positrons and electrons would show flux intensity peaks at Heliographic longitudes separated by approximately about 30°. An unambiguous positron measurement at the $\sim$10% level, achievable using PICAP, would be able to determine if this model prediction is correct.

2.3. Positrons in solar energetic particle events

Understanding the production of high energy ($\geqslant$5 MeV), charged particles by the Sun and in the Heliosphere is a clear goal of Solar and Heliospheric Physics research. The most credible models of $>$5 MeV charged particle production in SPEs involve the acceleration of a low energy seed population through some method, either through shocks or stochastic processes (e.g. Refs. [19,20]). When seeking to fit data to models, one of the most difficult problems is that of sorting the different particle populations correctly. Protons, which are the dominant source of charged particle energy density must be treated self-consistently, as they can be part of the initial seed population, or generated through secondary interaction early in the event, and can be one of the prime generators of wave turbulence during the event. Thus, for a model to accurately predict the proton energy spectra and time–intensity profiles, it is necessary to have the most accurate set of model parameters possible. Parameters such as the hydrogen density, B-field strength and configuration and temperature must be determined. As these parameters vary from flare to flare, as more information is made available, Solar flare models will become more accurate—the inclusion of positron fluxes is another channel through which these studies can be made.

One of the unique identifiers for high-energy charged particle acceleration in SPEs is the 511 keV positron annihilation line. The strength of this line depends on the number of positrons created during the event—less those that escape the Sun. Positrons do not normally occur in measurable quantities and are not part of an ambient seed population in the Sun. They are unique among observable stable particles as they are formed only as secondaries from high-energy charged particle interactions during SPEs. (Neutrons have similar production processes, but are unstable.) The 511 keV line was first reported for the August 4, 1972 flare [21], and observed since (e.g. Ref. [22]). As positrons are created only during the energization processes in SPEs, their production depends on the very parameters needed as input to the acceleration models. Thus, an accurate measure of the total positron flux would be useful to constrain these models. However, using the strength of the 511 keV annihilation line alone to infer the level of positron production involves numerous additional model dependent assumptions—as one of the loss processes, positron escape from the Sun, has yet to be measured. Also positron production in the Solar atmosphere will lead to not only the 511 keV line but also the 3-γ continuum (normally forbidden) to lower energies. As the strength of the line and continuum signals depend on the conditions where the positrons are formed, it is difficult, using the γ-ray measurements alone, to fully constrain the plasma and magnetic field parameters for any particular flare. The addition of a direct positron signal, or lack thereof, will help improve Solar flare models. Also, as the 511 keV line will occur as background in any γ-ray instrument, a direct measure of the energetic positrons can eliminate ambiguity when the 511 keV line is weak.

Positron production in large SPEs occurs through two channels, π^+ decay and β^+ emission from unstable isotopes formed in p and α interactions with ambient material (or heavy ion interactions with ambient H and He) in the Solar photosphere and corona. As β^+ emission occurs at hundreds of keV, and because below a few MeV there is almost no possibility of positron annihilation in flight (e.g. Ref. [23]), effectively all of the positrons formed via β^+ emission in the photosphere or chromosphere will eventually form positronium and be available for the formation of the narrow-band 511 keV line and the 3-γ continuum. However, positrons formed via π^+ decay start with initial energies in the range 10's–100's of MeV, and often do not slow down to energies low enough to contribute to the positronium annihilation line. Some of the high-energy positrons (>2 MeV) will either escape the Sun (unmeasured) or annihilate in-flight, emitting continuum γ-rays of relatively high energy, thus contributing to the $\geqslant 10$ MeV continuum [23]. Depending on model assumptions, the fraction of positrons surviving to energies below $\sim$2 MeV is between $\sim$0.75 and 0.9 [24]. Once they reach energies below $\sim$2 MeV, positron loss is dominated by the formation of positronium followed by annihilation. Model predictions for the photon/positron ratio, for positrons below a few MeV in energy, due to positronium decay in SPEs, can vary in the range 0.4–0.8, again depending on model assumptions (e.g. Ref. [25]). Uncertainties in fit quantities can give a range for the ratio of photons measured in the narrow-band 511 keV line to total positron production that may vary from $\leqslant$0.25 to $\geqslant$0.75. For example, calculations of positron production, and fits to the 511 keV line, in real SPEs (e.g. June 3, 1982), indicate that there are about equal numbers of positrons from β^+ emission and π^+ decay, but that there is a different time dependence associated with each of these processes [24]. The number of parameters in the models and their large range of variability make it difficult to find a unique set of parameters, using the γ-ray data alone, for any particular event. We note that the energy just above which model predictions indicate that escape from the Solar envelope is a meaningful process, $\sim$2 MeV, is just that energy range at which our PICAP instrument will operate. The addition of a measurement of the escaping $\geqslant$2 MeV positrons would give modelers additional data crucial to properly interpreting the 511 keV γ-ray line emission during SPEs.

The inclusion of positron measurements in a study of SPEs will open new channels for which studying γ-ray and radio emission is only an indirect proxy—that of direct magnetic connection to a flare site for energetic particle escape. The association of Type III radio bursts with Hα emission, ^{3}He-rich SPEs and X-ray events (e.g. Ref. [26]) has led to general association that a Type III burst indicates a magnetic connection between the flare site where electrons are energized and the interplanetary medium where the Type III burst is generated. While models indicate that this process can be reasonably explained (e.g. Ref. [27]), it remains the case that, because of the large numbers of sources for electrons, the electrons which create the Type III burst cannot be traced directly back to high energy interactions at the flare site. A positron signal seen in association with a flare, however, must indicate that there is some magnetic connection between the acceleration site and the interplanetary medium, so a Type III burst associated with a positron signal would indicate one set of magnetic morphologies while a Type III burst without an associated positron signal would indicate a different set of magnetic morphologies at the flare site.

As positrons have two general sources for production—through the creation of unstable isotopes which are β^+ emitters and through π^+ decay—a positron signal can be used to help map out the properties of the acceleration site for high-energy particles on the Sun. As particles are accelerated and gain in energy, isotopes such as ^{11}C, ^{13}N, ^{15}O, ^{19}Ne, etc. [28] will be created through nuclear interactions with the Solar material. These isotopes can decay through β^+ emission giving positrons with energies above $\sim$1 MeV. As the source spectrum hardens, π^+ production will begin. This will give an increase in higher energy positron production (through π^+ decay). If acceleration at the Sun hardens the spectrum even further, the onset of production of π^- and π^0 will act to level off or decrease the positron flux. A study of the time evolution of the positrons, looking for changes in their absolute flux, will allow for an independent measure of the acceleration occurring at the flare site.

The development of a new space-worthy technique for identifying positrons and separating them from negatrons will be a useful tool for future Solar observing missions. The addition of accurate positron data to other charged particle data can be used by modelers to aid in our understanding of how Solar flares accelerate particles near the Sun and how these accelerated particles are transported to the Earth.

3. PICAP

3.1. PICAP concept

Fig. 1 shows a specific design example that demonstrates the basic PICAP concept. The opening aperture is defined by three Si solid-state detectors, D1 (50 μm thick), and D2 and D3 (both 200 μm thick). Below is a central plastic scintillator, C, where electrons in the energy interval of interest will generally stop. A fourth Si detector, D4, identifies charged particles that exit the bottom of the instrument. Surrounding C is a torus of CsI scintillator divided into quadrants (G1, G2, G3 and G4 as shown in Fig. 2). Each segment forms an individual detector. The G detectors serve mainly to detect 511 keV annihilation photons from positrons stopping in C. They also work in conjunction with the plastic scintillator anti-coincidence shield (S), which will detect side-entering particles.

The PICAP design in Fig. 1 was the result of modeling a number of designs using a Monte-Carlo program incorporating the EGS4 electromagnetic shower code. The mass of the detector components is $\sim$1.5 kg, so a telescope with structure would mass $\sim$2 kg. We estimate a mass for the electronics with enclosure of $\sim$2 kg, giving a total instrument mass of $\sim$4 kg (see Section 3.6).

3.2. Electron response

The first requirement for PICAP is the efficient identification of positrons and negatrons as electrons, while effectively discriminating against other particle species, particularly protons.

Electrons with energies of $\sim$2–10 MeV within the acceptance cone of the instrument will generally trigger D2 and D3 but not D1 and deposit their residual energy in C. Electrons are distinguished from more massive particles of the same total energy by their much lower dE/dx which generates no trigger in D1 (the energy deposition being below a set threshold) and by small signals in D2 and D3. In contrast, a heavy particle (say a proton) stopping in C with comparable residual energy will trigger

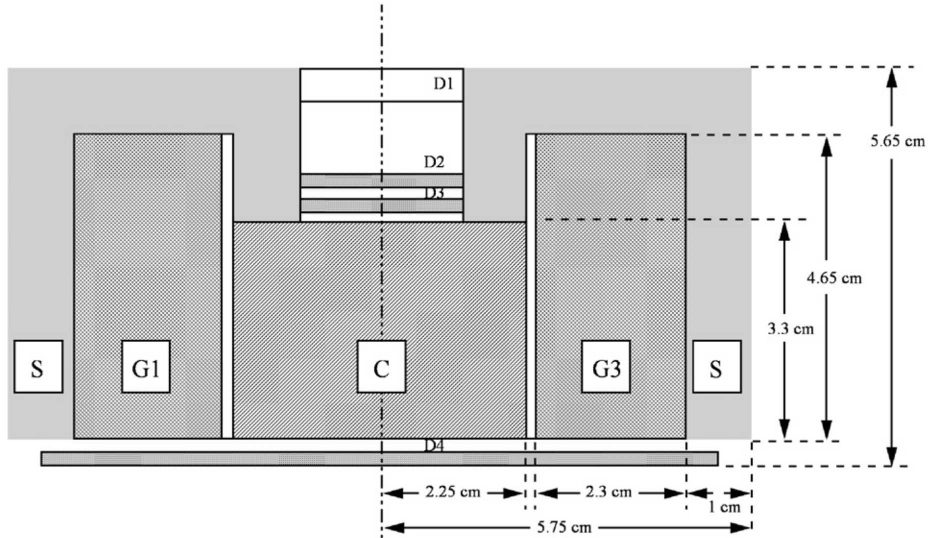

Fig. 1. Baseline design for the PICAP prototype. The opening aperture is defined by three Si detectors (D1–3). Below them is a central plastic scintillator (C) surrounded by a torus of four CsI scintillators (G1, G2, G3 and G4). A fourth Si detector (D4) and a plastic scintillator shield enclose the detector stack.

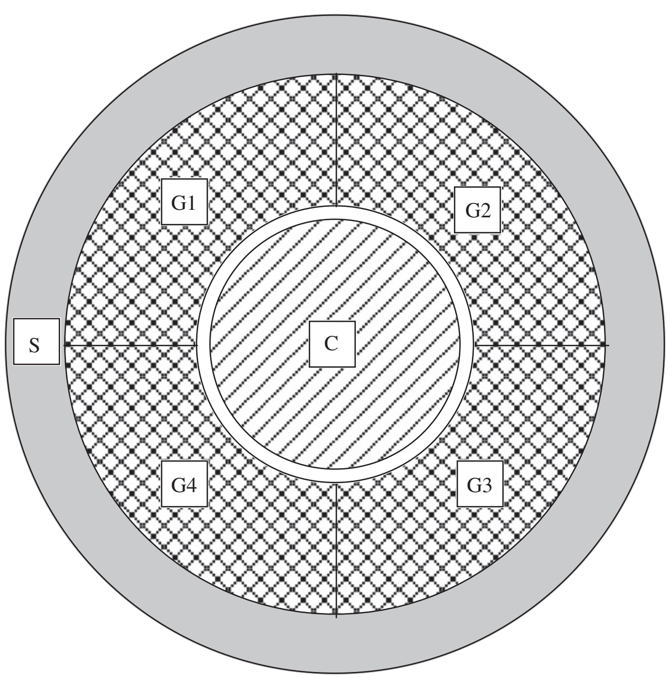

Fig. 2. Schematic cross section of the baseline PICAP instrument showing the segmentation of the CsI torus into four independent detectors (G1, G2, G3 and G4).

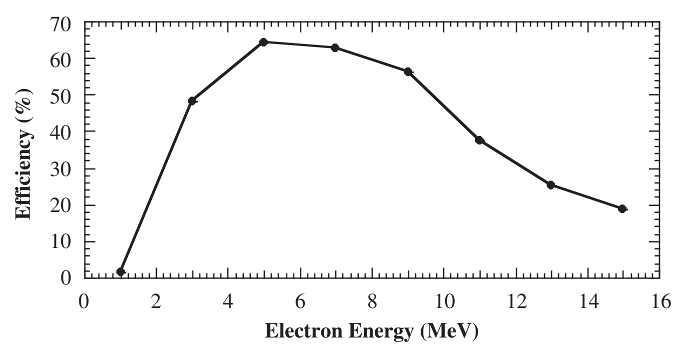

Fig. 3. Electron (in this case, negatron) detection efficiency of the baseline design as a function of incident energy using Monte-Carlo/EGS4 data.

D1 and deposit far more energy in D2 and D3. Relativistic protons will produce a dE/dx signature similar to an electron, but will not stop in C. Thus, the C signal will be too small, while D4 or S will trigger. The energy losses measured in D1, D2 and D3, together with the energy measurement in C will determine the particle total energy. The purpose of the redundant dE/dx measurements is to efficiently reject the usually much more abundant protons from the electron detection channels.

Fig. 3 shows the electron (in this case, negatron) detection efficiency of the baseline design as a function of energy using Monte-Carlo/EGS4 data. At low energies, the efficiency declines as events fail to reach C. In contrast to more massive particles, electrons have a significant elastic scattering probability, thus some 2 MeV electrons will reach C, while others will stop above C. Similarly, for high energies, the efficiency declines as electrons begin reaching D4. In the middle energy region of the plot, the majority of electron events that were rejected have scattered into S or a G detector.

It is important to emphasize that the main science goal of PICAP is to measure the positron *fraction*. To this end, it is important to measure both positron and negatrons with the same instrument, thus reducing systematic effects. The response of D1, D2, D3 and C to electrons is nearly identical for positrons and negatrons. The main difference in overall PICAP response arises from annihilation photons created when positrons stop in C. In a small fraction of these events, annihilation photons will trigger S or deposit other than 511 keV in a G segment. Thus, the identification efficiency of positrons as electrons is slightly lower than for negatrons.

One subtle effect noted in the modeling is that positrons of the same kinetic energy on an average result in a higher measured energy in an instrument as some of the energy from the annihilation photons can contribute to the measured energy. This effect may have implications for existing electron measurements.

It should be noted that our electron identification technique is quite conventional. It has been used widely on instruments flown on such missions as IMP-8, *Pioneer*-10 and -11, *Voyager*-1 and -2, *Ulysses* and others, which gives us a high level of confidence in its effectiveness.

3.3. Positron response

Positrons—as opposed to negatrons—stopping in C will annihilate, producing two 511 keV photons going in opposite directions from the point of annihilation. Plastic scintillator is used for C because it is relatively transparent to 511 keV photons. Similarly, CsI was chosen for the G detectors to increase the likelihood of annihilation photons being detected in G segments. (Other kinds of high-density scintillators are possible alternatives.) The requirement for positron detection is the same as for negatrons, plus the detection of annihilation photons (defined as a 511 ± 25 keV signal) in *exactly two* different G segments with no signals above threshold (0.1 MeV) in any other G, or in S. Fig. 4 shows the detection efficiency for the baseline PICAP instrument. As can be seen in the figure, ~1% of positrons in the energy interval 3–8 MeV are so identified.

The shape of the efficiency plot is largely determined by the geometry of the G segments. For example, in the baseline design, the torus projects above the top of the C detector. This is required to extend the positron sensitivity to low energies. If the torus were level with the top of C, the detection efficiency for positrons stopping at the top of C would be nil as one of the annihilation photons—purely by geometry—would pass above the torus, even if the other were detected. Similarly, the drop off in sensitivity at high energies results from the same effect for positrons stopping at the bottom of C. The goal of this design was to provide a reasonably flat response for 5–10 MeV positrons. For other energy intervals, a different geometry would be used.

Of equal importance to the efficiency of positron detection is the rejection efficiency of negatrons from the positron channel. Monte-Carlo/EGS4 data with 10^6 negatrons at 9 MeV produced only 12 false positrons. (Meaning, the 9 MeV negatrons appeared to be ~8 MeV positrons by depositing ~500 keV in two G detectors.) Thus, 10^5 electron events with an actual 10% positron fraction would produce ~101 events in the instrument's positrons channel. From this, ~1 event would be subtracted as negatron background, yielding a measured positron fraction of $10 \pm 1\%$. Naturally, if the positron fraction were greater, the same level of precision would be obtained with a proportionately lower total number of events.

The requirement of two 511 keV signals in exactly two different G's is extremely stringent. It is, however, crucial: ~0.4% of negatrons will scatter into a G segment producing a single 511 ± 25 keV signal. Even taking into account the fact that a larger fraction of actual positron events will produce a single 511 keV signal (~10%), the negatron background level is problematic. Using the previous example of 10^5 events with a 10% positron fraction, a single- (rather than double-) photon requirement would yield ~1400 events identified as positrons, of which ~400 would be negatron background. Thus, while a single-photon requirement increases the detection efficiency by a factor of ~10 compared to the two-photon requirement, it also has a background that is a factor ~400 greater. Clearly, even a modest systematic in the background subtraction would produce a systematic error in the measurement of the positron fraction comparable to the statistical error. This also explains why the CsI torus is segmented: scattered negatrons can just as well deposit 1022 keV in a solid CsI torus; they are far less likely to deposit exactly half of that energy in two different segments.

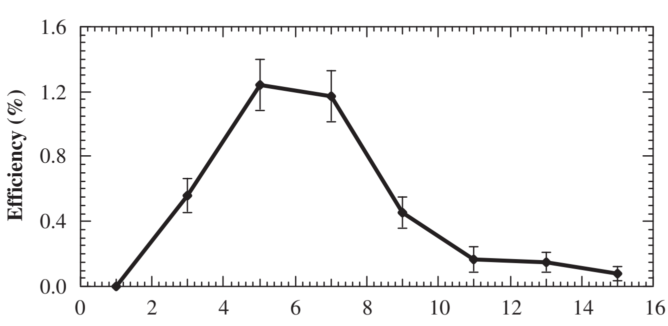

Fig. 4. Positron identification efficiency of the baseline PICAP instrument requiring that both annihilation photons be detected in two different CsI torus segments.

While a single-photon identification requirement is inferior in terms of rejecting false positrons compared to the double photon requirement, this is not to imply that it should be ignored. In an actual mission, the two methods would be complementary, with the two-photon method providing a clean calibration for the single-photon method under the actual flight conditions. This would thus include all sources of background, accidentals from photons produced in the spacecraft itself being a prime example.

3.4. Background concerns

Background is always a major concern when measuring rare species (positrons, in this case) in the presence of much larger fluxes of similar species (negatrons) and larger still fluxes of other radiations (protons, etc.). The discrimination between negatrons and positrons, being fundamental to the PICAP concept, particularly the use of two coincident 511 keV photon detections, was addressed earlier. The Monte-Carlo results clearly demonstrate the effectiveness of PICAP in this regard.

Protons are a major source of background in magnet spectrometers. A proton misidentified as an electron will bend in the same direction as a positron, and thus be so counted. In a PICAP instrument, a proton would not only have to be misidentified as an electron but would also have to produce 511 keV signals in two G detectors to be misidentified as a positron—an extremely unlikely case. A π^+ produced in the instrument will either escape, or decay to a muon that escapes. Inelastic proton collisions with nuclei in the C detector will—rarely—produce β^+ unstable nuclides (for example, ^{11}C, ^{12}C, ^{10}C or ^{12}N) but the half-lives of the resulting isotopes (20.3 min for ^{11}C, 19.3 s for ^{10}C and 11 ms for ^{12}N) would be far longer than the coincidence window (~few μs, limited by the CsI) of the instrument, excluding such already rare events at the $>10^{-6}$ level. Thus, in PICAP, any proton contamination will be to the total electron channel, not the less abundant positron channel.

Another obvious concern is γ-rays produced in the spacecraft. While a full exploration of this issue would require modeling beyond the scope of the present work, PICAP has some obvious advantages in this regard over previous instruments.

Accidental coincidences between a negatron and an annihilation γ-ray from the spacecraft are possible. The photons can arise from both β^+ emitters produced by inelastic collisions in the spacecraft, or stopping cosmic ray positrons. This constituted a significant background for the OGO-5 measurement, despite the instrument being placed on a boom [4]. In the case of PICAP, it is important to note that as annihilation photons go in opposite directions, a positron annihilating anywhere outside the G torus can only produce a single 511 keV signal—by the geometry, the other photon will miss the instrument. Thus, it requires photons from two, not one, separate events (nuclear decay or stopping cosmic ray positron) in the spacecraft, both interacting in different G detectors within the coincidence window of a negatron, to produce a false positron signal. Triple accidentals are far less likely than the double accidentals on OGO-5, which nonetheless was able to obtain a measurement. This reduced susceptibility to background from the spacecraft is an advantage of the PICAP technique.

While a PICAP instrument is less susceptible to accidentals, any such instrument would be designed to monitor the rate of 511 MeV signals in the G detectors, both single photon and two photons, that are not coincident with electrons. These data would be a monitor, and useful in correcting for accidental coincidence events.

At higher energies, γ-rays can pair produce in the plastic scintillator, C. If the positron remains in C and annihilates, while the negatron exits through the aperture, a false positron signal could result. While modeling would be required to fully address this concern, it should be noted first, that if the negatron has sufficient kinetic energy to escape through the solid-state detectors and be identified at an electron, it is far more likely the positron will also escape the C detector into a surrounding detector, thus invalidating the event. It is only the case where the positron remains in C that the γ-ray event will be identified as a positron. Furthermore, the geometry of the instrument makes it far more likely that the negatron will miss the aperture, triggering detectors other than D2 and D3, again invalidating the event. (In the case of the design in Fig. 1, C has a surface area of 78.4 cm^2 while D3 has an area of 5.3 cm^2, so only 6.8% of such events would hit D3, and most of those would be at too wide an angle and thus also trigger S, invalidating the event.) Again, using the G detectors to monitor the γ-ray background would, together with modeling information, help correct for any such background.

Finally, PICAP was inspired by a measurement of the β^+ partial half-life of ^{54}Mn [29] at Argonne National Laboratory. One author was a participant owing to his interest in cosmic-ray chronometry. ^{54}Mn has a half-life of 312.4 days with electron capture being the dominant decay branch. Wuosmaa et al [29]. measured the β^+ branching ratio to be $(1.2 \pm 0.26) \times 10^{-9}$ using the APEX positron spectrometer [30]. APEX identified positrons by a triple coincidence between electrons stopping in Si detectors and two 511 keV annihilation photons detected in NaI scintillators. The branching ratio for β^- was calculated to be $\sim 10^3$ larger than for β^+. With respect to PICAP, the significance of the APEX experiment was its ability to identify positrons in a 10^3 larger flux of negatrons and a 10^9 larger flux of X-rays.

3.5. Design considerations

The most obvious design consideration in PICAP is that the number of annihilation photons detected increases rapidly with the thickness of CsI used in the G detectors. To first order, based upon our modeling to date, the two-photon positron detection efficiency goes as $(1-e^{-kx})^2$ where x is the thickness of G and $k = 0.29\,\mathrm{cm}^{-1}$ for typical PICAP geometries. Thus, doubling the CsI thickness for the baseline instrument would improve the detection efficiency by a factor of 2.3. The penalty is mass: the CsI torus constitutes 1 kg of the 1.5 kg total detector mass in the baseline instrument. Doubling the thickness would more than double the torus mass. The goal for the baseline detector was a positron detection efficiency of $\sim$1% with an instrument mass suitable for a space mission. Naturally, the torus thickness could be increased for missions where instrument mass is less constrained.

The baseline instrument has the CsI torus divided into four equal segments. A larger number of segments would slightly increase the detection efficiency. Our modeling indicates that the gain is slight and not justified in view of the increased complexity of the instrument and associated electronics.

The energy interval of a PICAP instrument could be extended by increasing the height of the central scintillator. In order to significantly lower the minimum energy response, we would decrease the thickness of the D2 and D3 detectors. The only electronic design restriction on decreasing the detector thicknesses is that of signal-to-noise in the charge pulse from the detectors. For an actual flight instrument, decreasing the D2 and D3 detector thicknesses would increase the absolute flux of particles into the plastic scintillator, which might dictate a smaller geometry factor to avoid pulse pile-up during large Solar events. (Smaller area detectors would also reduce capacitive noise, perhaps facilitating in turn thinner detectors.)

A potential benefit to lowering the positron detection threshold is the opportunity to measure positrons from the various inverse-β radionuclides with emission below 1 MeV that can be formed in processes associated with Solar flares and SPEs (Section 2.3). As the formation of different isotopes is dependent on conditions in the Solar atmosphere, which differ from those that create pion-induced positron emission, the capability to distinguish these sources might well be scientifically desirable, in which case a PICAP instrument would be designed to have its energy response curve extend to lower energies.

As emphasized earlier, the PICAP concept is quite flexible as to energy and application and can be optimized for different mission profiles and goals.

3.6. Event rate considerations

Because of PICAP's excellent proton and electron rejection from the positron signal, it is only the detection efficiency of positrons themselves that drives the precision of the positron/negatron ratio, which can be derived. To estimate the measurement capabilities of a PICAP instrument in-flight, we use our design and reasonable assumptions on the positron and electron fluxes in the Heliosphere. The baseline flight design, which we have detailed in Fig. 1 and Tables 1 and 2, has a geometrical factor of $\sim$3 cm^2 sr over the electron measurement range 2–10 MeV.

As the steady-state electron flux in the Heliosphere over this energy range is $\sim$2 particles/(m^2 sr s MeV) [31], our baseline flight design would detect electrons, in the energy interval 2–10 MeV, at a rate of 0.0048 particles/s. While never having been measured at these energies, theoretical limits indicate that the positron fraction levels off toward low energy at between 10% and 20% (e.g. Ref. [8]). Given our PICAP design's positron efficiency of $\sim$1%, we would expect to observe 100 positrons, thus making a measurement with 10% statistical precision, in about 240 days. This would of course vary as a function of the Solar cycle. As the time scale for Solar modulation over which we would expect to

Table 1
Estimated mass budget

Components	Mass (kg)
10 Electronics boards (70 g each)	0.700
Motherboard with connectors	0.210
Power converter board	0.180
Four solid-state Si detectors (D1, D2, D3, A)	0.020
Central plastic scintillator (C)	0.053
Four quarter-torus CsI scintillators (G1-4)	1.092
Anti-coincidence plastic scintillator	0.285
Al mountings/housings for detectors	0.064
Six PMT's with housings (75 g each)	0.450
Hardware and fasteners	0.040
Window with support	0.025
Enclosure	0.525
Sub-total	3.644
15% contingency	0.546
Total	4.190

Table 2
Estimated regulated power budget

Board	Power (W)
Six analog (375 mW each)	2.25
ADC	0.19
Logic	0.12
Sub-total	2.56
15% contingency	0.39
Total	2.95

see charge-sign effects is approximately 11 years, making high precision positron measurements on time scales of under 1 year is a reasonable goal for a space-based instrument.

In the presence of a shock or during other enhanced rate periods, when the absolute flux of electrons increases by factors of 10's to 1000's over the steady-state intensity described earlier, the time necessary to make a precision measurement of the positron fraction would decrease accordingly. Thus our baseline flight PICAP instrument will also be able to make useful positron measurements on time scales associated with CIRs and Solar particle events. During impulsive SPEs, the electron flux is generally above 1 particle/(cm^2 sr s MeV) and can go as high as 100 particles/(cm^2 sr s MeV). Taking the higher flux, if we assume a positron fraction of 0.1% (well below the limit of 6×10^{-3} from the EIS; Refs. [2,3]), we will be able to make a 10% statistical measure of the positron fraction in $\sim$12 h.

To date, the only medium energy positron detection for a Solar event was from the Helios E8 instrument [6]. While a PICAP instrument would operate at higher energies, say 1–3 MeV as opposed to 152–546 keV for E8, absent more directly applicable measurements, it is worth considering their estimated flux. If we take their estimated 1 AU flux, we get a differential flux of 0.71 e^+/(cm^2 sr s MeV), which would result in a detection rate in the baseline PICAP instrument of $\sim$0.05 e^+/s, permitting a 10% measurement in $\sim$30 min. Unlike the E8 instrument, a PICAP instrument can make positron measurements throughout the Solar event, so a clear detection would result.

If instrument mass is not a significant constraint for a given mission, a larger instrument and/or a higher detection efficiency for positrons (attained by increasing the thickness of the CsI torus as discussed in Section 3.4) is also possible. In most applications, the latter would probably be preferred. Increasing the size of the instrument affects only the mass and size; the power required to run a larger instrument would not increase significantly from our baseline estimations.

3.7. Ion response

While the baseline instrument is optimized for electron measurements, it is inherently capable of measuring ions with the dE/dx versus residual energy technique. For ion events stopping in C, the baseline instrument would easily separate H, ^{3}He, ^{4}He. Given sufficient dynamic range in the linear electronics, elements in the C, N and O region should be separable and a measurement of the Fe group (though not individual elements) would be possible. Obviously, these measurements would be of value for SEP studies and also for GCR modulation studies. The primary limitation on the heavy ion separation would be variations in the thickness of detector material traversed in D1–D3 with angles of incidence. A trajectory determining system (such as position sensing detectors or inclined sensors; [32,33]) could be added to improve elemental resolution. Whether such additional complexity would be justified would depend upon a particular mission profile and scientific goals. In the case where a separate ion instrument is on-board, the availability of H and He measurements in a PICAP instrument would be of enormous value for inter-calibration.

3.8. Neutron and γ-ray response

A standard method of detecting neutral particles in space is a detector surrounded by an anti-coincidence system to exclude charged particle events. Both the C and G detectors in a PICAP instrument are effectively surrounded by detectors that, in logic, can be used for anti-coincidence. Plastic scintillator has a relatively good response to energetic neutrons due to scintillation from scattered proton; it has a relatively poor response to γ-rays owing to the low atomic number of its constituents. The exact converse applies to CsI scintillator. Thus, in a PICAP instrument, a signal in C with no other detectors triggering would most likely be the result of an energetic neutron, while a signal in a G segment with no other detectors triggering would most likely be the result of a γ-ray. If the response efficiencies of both these detection channels to γ-rays and neutrons were determined, a PICAP instrument could provide a useful measurement of both radiations with no modification to the telescope and only a modest increase in the complexity of the electrons.

3.9. Resource budgets

Mass and (regulated) power budgets for our baseline instrument are given in Tables 1 and 2, respectively. The instrument enclosure would be a (generous) 1-mm-thick aluminum box of dimensions $18\,cm\times18\,cm\times18\,cm$. The mass budget is broken down by major component, and the power budget is broken down by board. Both our estimated mass and regulated power budgets include 15% contingency (as noted). Thus, a working space instrument would mass about 4.2 kg and use about 3 W regulated power. While these are estimates, they are in line with charged particle instruments, which have been and are currently in operation.

4. Conclusions

Measurements of moderate energy positrons in space would provide new and valuable information on cosmic ray propagation and modulation (particularly charge-sign effects) and SEP events. Such measurements would constrain and test a range of important astrophysical, Heliospheric and Solar models.

PICAP offers an extremely simple method to achieve such measurements that is well suited to deep space missions. Compared to magnetic spectrometers, PICAP offers lower mass and power requirements and avoids the need for complex particle tracking systems with their associated electronics. Modeling of our baseline PICAP instrument shows that useful measurements are possible with a 4 kg instrument giving positron detection efficiency of $\sim$1%. A PICAP instrument can be optimized to a variety of mission constraints and energies intervals. For example, a moderate increase in the CsI detector mass by $\sim$1.5 kg (still reasonable even for a deep space mission) would increase that efficiency to $\sim$2.5%.

Future work should include additional modeling to further address background concerns, including background resulting from a spacecraft.

Disclaimer

The views expressed herein are those of the authors and do not reflect the position of the United States Military Academy, the Department of the Army, or the Department of Defense.

References

[1] P. Picozza, et al., Astroparticle Phys. 27 (2007) 296.
[2] G.J. Hurford, R.A. Mewaldt, E.C. Stone, R.E. Vogt, in: Proceedings of the 13th International Cosmic Ray Conference, Denver, CO, vol. 2, 1973, p. 1613.
[3] R.A. Mewaldt, E.C. Stone, R.E. Vogt, in: Proceedings of the 14th International Cosmic Ray Conference, Munich, West Germany, vol. 5, 1975, p. 1668.
[4] T.L. Cline, G. Porreca, in: Proceedings of the 11th International Cosmic Ray Conference, Budapest, vol. 1, 1969, p. 145.
[5] T.L. Cline, E.W. Hones Jr., in: Proceedings of the 11th International Cosmic Ray Conference, Budapest, vol. 1, 1969, p. 159.
[6] E. Kirsch, E. Keppler, K. Richter, in: Proceedings of the 19th International Cosmic Ray Conference, La Jolla, CA, vol. 4, 1985, p. 158.
[7] E. Keppler, et al., J. Geophys. 42 (1977) 633.
[8] J.K. Daugherty, R.C. Hartman, P.J. Schmidt, Astrophys. J. 198 (1975) 493.
[9] S.W. Barwick, et al., Astrophys. J. 498 (1998) 779.
[10] R.J. Protheroe, Astrophys. J. 254 (1982) 391.
[11] I.V. Moskalenko, A.W. Strong, Astrophys. J. 493 (1998) 694.
[12] E.N. Parker, Planet. Space Sci. 13 (1965) 9.
[13] J.R. Jokipii, E.H. Levy, W.B. Hubbard, Astrophys. J. 213 (1977) 861.
[14] J.R. Jokipii, E.H. Levy, Astrophys. J. Lett. 213 (1977) L85.
[15] J.M. Clem, P. Evenson, D. Huber, K.R. Pyle, C. Lopate, J.A. Simpson, J. Geophys. Res. 105 (2000) 23099.
[16] P. Evenson, D. Huber, E. Tuska-Patterson, J. Esposito, D. Clements, J. Clem, J. Geophys. Res. 100 (1995) 7873.
[17] J. Kota, J.R. Jokipii, EOS Transactions of AGU, Spring Meeting, Baltimore, 25–27 May 1997.
[18] J.R. Jokipii, J. Kota, in: Proceedings of the 26th International Cosmic Ray Conference, Salt Lake City, UT, vol. 6, 1999, p. 504.
[19] D.V. Reames, Space Sci. Rev. 90 (1999) 413.
[20] H.V. Cane, W.C. Erickson, J. Geophys. Res. 108 (A5) (2003) SSH-8.
[21] E.L. Chupp, et al., Nature 241 (1973) 333.
[22] M. Yoshimori, S. Nakayama, H. Ogawa, in: Proceedings of the 27th International Cosmic Ray Conference, Hamburg, Germany, vol. 8, 2001, p. 3025.
[23] R. Ramaty, R.J. Murphy, B. Kozlovsky, R.E. Lingenfelter, Sol. Phys. 86 (1983) 395.
[24] R.J. Murphy, C.D. Dermer, R. Ramaty, Astrophys. J. (Suppl.) 63 (1987) 721.
[25] B.L. Brown, M. Leventhal, A.P. Mills Jr., D.W. Gridley, Phys. Rev. Lett. 53 (1984) 2347.
[26] D.V. Reames, R.G. Stone, Astrophys. J. 308 (1986) 902.
[27] I. Roth, M. Temerin, Astrophys. J. 477 (1997) 940.
[28] G.H. Share, R.J. Murphy, Astrophys. J. 452 (1995) 933.
[29] A.H. Wuosmaa, et al., Phys. Rev. Lett. 80 (1998) 2085.
[30] I. Ahmad, et al., Nucl. Instr. and Meth. A 370 (1996) 539.
[31] E.S. Ferreira, M.S. Potgeiter, R.A. Burger, B. Heber, H. Fichtner, C. Lopate, J. Geophys. Res. 106 (A12) (2001) 29313.
[32] J.J. Connell, C. Lopate, R.B. McKibben, Nucl. Instr. and Meth. A 570 (2001) 399.
[33] J.J. Connell, C. Lopate, R.B. McKibben, A. Enman, Nucl. Instr. and Meth. 457 (2007) 220.